Critical behaviour of the two-dimensional EA model with a Gaussian bond distribution

1992 J. Phys. A: Math. Gen. 25 4985

(http://iopscience.iop.org/0305-4470/25/19/013)

J. Phys. A: Math. Gen. 25 (1992) 4985–5003. Printed in the UK

Critical behaviour of the two-dimensional EA model with a Gaussian bond distribution

N Kawashima, N Hatano and M Suzuki

Department of Physics, Faculty of Science, University of Tokyo, Hongo, Bunkyo-ku, Tokyo 113, Japan

Received 31 March 1992

Abstract. The spin-glass susceptibility of the two-dimensional EA model is investigated by the numerical transfer-matrix method. It is found that the droplet picture gives a fairly good description of the critical behaviour. The critical exponent $\theta \equiv -1/\nu$ is estimated as $\theta = -0.48(1)$, both through finite-size scaling and through the coherent-anomaly method (CAM). The present estimate is consistent with our previous estimate $\theta = -0.476$. These values do not, however, agree with the stiffness-exponent estimate θ_S through the domain-wall scaling. This disagreement suggests that the assumption $\theta = \theta_S$ in the domain-wall scaling does not hold.

1. Introduction

Although the spin-glass problem has attracted interest from many researchers, the nature of the low-temperature phase of finite-dimensional spin-glass systems remains unclarified. For instance, it has not been settled yet whether the $P(q)$ of Parisi has non-trivial structure for the three-dimensional $\pm J$ model below the critical temperature. There are two main pictures of it which may explain correctly the low-temperature phase of the model. One is the mean-field picture, according to which we can obtain numerous thermodynamic states and the non-trivial structure of $P(q)$. This picture also suggests the existence of a phase transition in the presence of a magnetic field. The other is the so-called droplet picture [1]. In this picture there is only one pair (or, at most, a finite number of pairs) of thermodynamic states, and $P(q)$ consists of a finite number of δ-peaks. In addition, the phase transition is considered to be absent in the presence of a uniform field in contrast to the mean-field picture. Besides these two pictures, some numerical evidences suggest another possibility. For example, several numerical calculations [2–5] show that the variance of $P(q)$ may be vanishing even in the case where $T < T_c$ and $H = 0$.

As for the two-dimensional Edwards–Anderson (EA) model with a symmetric bond-distribution, few researchers doubt that a finite-temperature phase transition does not occur. A number of numerical works have been done on the criticality of the two-dimensional $\pm J$ model at $T = 0$. For the $\pm J$ model, numerical calculations [6] have given several estimates for the exponents ν, η and γ_{SG}, which are consistent with each other.

As for the two-dimensional model with a Gaussian bond distribution, there is disagreement between estimates of the exponent ν so far obtained. In the domain-

0305-4470/92/194985+19$04.50

wall-scaling argument [7], the absolute value of the stiffness exponent θ_S which characterizes the size dependence of the domain-wall energy is assumed to be equal to the inverse of the critical exponent ν. The domain-wall energy here is defined by the difference in ground-state energies of two systems which differ from each other only in their boundary condition, a periodic boundary condition is applied to one system and an antiperiodic boundary condition to the other. The index θ_S has been estimated through numerical calculations as follows [8, 9]:

$$-\theta_S = 0.291(2) \qquad [8] \tag{1.1}$$

$$= 0.281(5) \qquad [9]. \tag{1.2}$$

Estimation of $\nu(=-1/\theta)$ has also been done by calculating the largest eigenvalues in the even and odd eigenspaces of transfer matrices [10, 11]. The results are

$$\nu(=-1/\theta) = 2.96(22) \sim 1/0.34 \qquad [10] \tag{1.3}$$

$$= 4.2(5) \sim 1/0.24 \qquad [11]. \tag{1.4}$$

It should be noted that all the above estimates are not based on direct calculations of macroscopic physical quantities, or derivatives of the free energy. Recently, two of the present authors calculated [12] zero-temperature magnetization for various strength of the magnetic field. The finite-size scaling analysis on the resulting data yielded

$$-\theta = 0.476(5). \tag{1.5}$$

The same data yielded $-\theta = 0.51(4)$ when an additional correction term is included in the fitting function. All the above estimaes of θ apparently do not agree with each other within the limit of statistical error. Whether this disagreement is due to finite-size effect or due to a more essential reason is an interesting and difficult problem. The purpose of the present paper is to give new estimation of $-\theta$ which is based on direct measurement of a macroscopic physical quantity, namely, the spin-glass susceptibility χ_{SG}.

In this paper, we present two kinds of calculations. One is a calculation of the nonlinear magnetic susceptibility χ_2, which is equivalent to the spin-glass susceptibility in a vanishing field. The data are analysed with the finite-size scaling. The other one is a calculation of two-point spin-glass correlation functions of finite-size systems. The data are analysed in the framework of the double-cluster approximations (DCA) [13–15] combined with the coherent-anomaly method (CAM) [16]. Within the scope of Fisher's finite-size scaling for two-point correlation, these two calculations are essentially equivalent to each other, and the exponents obtained through them should relate directly to the scaling exponent of the free energy. Indeed, the estimates are fully consistent with each other, $-\theta = 0.48(1)$, and also agree with the estimate (1.5). This fact suggests that finite-size correction to scaling is not so large in the present calculations. The estimates, however, are not compatible with the results (1.1)–(1.4) by other groups.

2. Finite-size scaling and the droplet argument for nonlinear susceptibility

The critical behaviour of the present model is characterized by one-parameter scaling [7]. Although brief discussions about this problem have already been given in several articles [1, 7], let us review them for the sake of completeness.

We do not have any rigorous proof for the algebraic, or power-law singularity of various quantities. Nonetheless it seems to be reasonable to assume it, since we have much numerical evidence as mentioned in the introduction. Let us assume the following scaling form for an arbitrary quantity Q:

$$Q(T, H, L) = L^{\psi_Q} \tilde{Q}(TL^{-\theta}, HL^{-\phi}) \tag{2.1}$$

where T, H and L are the temperature, the magnetic field and the system size respectively. Here we have assumed the critical temperature is zero, $T_c = 0$. The scaling exponents θ and ϕ are believed to be independent of the quantity Q, because macroscopic physical quantities such as energy, specific heat, magnetization, magnetic susceptibility, nonlinear magnetic susceptibility [17], etc, can be derived from the free energy through differentiation with respect to T and/or H. There are several reports [18], however, that in some frustrated models which exhibit a chiral phase transition, the spin–spin correlation and chirality–chirality correlation are described by different thermal exponents, ν_s and ν_c, respectively. On the other hand, the exponent ψ_Q takes varying values for different quantities. Let us denote ψ_f simply by ψ, i.e.

$$f(T, H, L) = L^{\psi} \tilde{f}(TL^{-\theta}, HL^{-\phi}). \tag{2.2}$$

Here the symbol f denotes the singular part of the free energy per spin averaged over bond configurations. Two of the above exponents ψ, θ and ϕ are determined by the other under the two requirements below.

By differentiating f four times with respect to H, we get an expression for the nonlinear magnetic susceptibility χ_2

$$\chi_2(T, H, L) = -\frac{1}{6}\frac{\partial^4 f}{\partial H^4} = L^{\psi-4\phi} \tilde{\chi}_2(TL^{-\theta}, HL^{-\phi}). \tag{2.3}$$

Here we should note the following relation between the nonlinear susceptibility [17] and the spin-glass susceptibility at $H = 0$

$$\chi_2(T, 0, L) = \frac{\beta^3}{6N}[\langle M^4\rangle - 3\langle M^2\rangle^2]_J = \beta^3\left(\frac{2}{3} - \chi_{SG}\right) \tag{2.4}$$

where

$$M \equiv \sum_i S_i \tag{2.5}$$

and

$$\chi_{SG} \equiv \frac{1}{N}\sum_{i,j}[\langle S_i S_j\rangle^2]_J. \tag{2.6}$$

Here we have used the gauge invariance of the system. Thus we obtain the scaling form for χ_{SG} at $H = 0$

$$\chi_{SG}(T, 0, L) \sim -T^3 L^{\psi-4\phi} \tilde{\chi}_2(TL^{-\theta}, 0) \sim L^{\psi-4\phi+3\theta} \tilde{\chi}_{SG}(TL^{-\theta}, 0). \tag{2.7}$$

Now we should note that the following two facts yield two equations between θ, ϕ and ψ. Firstly, owing to the local gauge invariance, we have the following exact expression of the linear susceptibility

$$\chi(T,0,L) = \beta. \tag{2.8}$$

To make this expression consistent with the scaling form

$$\chi(T,H,L) = -\frac{\partial^2 f}{\partial H^2} = L^{\psi-2\phi}\tilde{\chi}(TL^{-\theta}, HL^{-\phi}) \tag{2.9}$$

we put

$$\gamma = (2\phi - \psi)/\theta = 1. \tag{2.10}$$

Secondly, we require the uniqueness of the ground-state pair, which is an immediate consequence of the continuity of the bond distribution. We have

$$\langle S_i S_j \rangle^2 = 1 \qquad \text{at} \qquad T = 0. \tag{2.11}$$

This leads to

$$\chi_{\mathrm{SG}}(0,0,L) \propto L^d. \tag{2.12}$$

Comparing this expression with (2.7), we have

$$\psi - 4\phi + 3\theta = d. \tag{2.13}$$

Thus we have obtained the 'one-parameter scaling' for χ_{SG}

$$\chi_{\mathrm{SG}}(T,H,L) \sim L^d \tilde{\chi}_{\mathrm{SG}}(TL^{-\theta}, HL^{d/2-\theta}). \tag{2.14}$$

Now many other critical exponents are expressed by a single exponent. The exponent γ_{SG} which describes the divergence of the spin-glass susceptibility

$$\lim_{L\to\infty} \chi_{\mathrm{SG}}(T,0,L) \propto T^{-\gamma_{\mathrm{SG}}} \tag{2.15}$$

is expressed in terms of θ as

$$\gamma_{\mathrm{SG}} = -d/\theta. \tag{2.16}$$

The scaling form for the magnetization is given by

$$m(T,H,L) = -\frac{\partial f}{\partial H} = L^{-d/2}\tilde{m}(TL^{-\theta}, HL^{d/2-\theta}) \tag{2.17}$$

$$\propto H^{1/\delta} \qquad (T = 0, L \to \infty) \tag{2.18}$$

with

$$\delta = 1 - 2\theta/d. \tag{2.19}$$

The limiting case, $T = 0$, of (2.17) has been used in the previous analysis [12]. In the present paper we use another limiting case, $H = 0$, of (2.14).

Next, let us see how the expression (2.7) is derived from Fisher's finite-size scaling for two-point correlations, for later convenience. The scaling form of two-point spin-glass correlation is written as follows

$$[\langle S_i S_j \rangle^2]_J \simeq R_{ij}^{-(d-2+\eta)} G(T R_{ij}^{1/\nu}) \tag{2.20}$$

where R_{ij} is the distance between the spins S_i and S_j. Here we have assumed $T_c = 0$ again. The spin-glass susceptibility is related with (2.20) as follows;

$$\chi_{SG}(T, 0, L) = \frac{1}{N} \sum_{i,j} [\langle S_i S_j \rangle^2]_J \simeq \sum_j [\langle S_0 S_j \rangle^2]_J$$
$$\simeq \int_0^L R^{d-1} \mathrm{d}R \frac{G(T R^{1/\nu})}{R^{d-2+\eta}} = L^{2-\eta} K(T L^{1/\nu}) \tag{2.21}$$

where the symbol S_0 denotes the central spin, and

$$K(x) \equiv x^{-(2-\eta)\nu} \int_0^x t^{(2-\eta)\nu - 1} G(t) \, \mathrm{d}t. \tag{2.22}$$

Comparison between (2.14) and (2.21) yields $K(x) = \tilde{\chi}_{SG}(x, 0)$ with

$$2 - \eta = d \qquad \text{and} \qquad 1/\nu = -\theta. \tag{2.23}$$

Now the correlation (2.20) is written in the form

$$[\langle S_i S_j \rangle^2]_J \simeq G(T R_{ij}^{-\theta}) \tag{2.24}$$

and the scaling function $\tilde{\chi}_{SG}(x, y)$ with $y = 0$ is given by

$$\tilde{\chi}_{SG}(x, 0) = x^{d/\theta} \int_0^x t^{-d/\theta - 1} G(t) \, \mathrm{d}t. \tag{2.25}$$

The asymptotic behaviour of $G(x)$ in the region $x \gg 1$ is known to be $G(x) \sim \exp(-k x^{\nu})$, where k is a positive constant. With the help of the droplet argument, the asymptotic behaviour in the region $x \ll 1$ can be predicted in the following form:

$$G(x) = 1 - cx + o(x) \tag{2.26}$$

where c is a positive constant. This leads to the expression

$$\chi_{SG}(T, 0, L) = L^d \tilde{\chi}_{SG}(T L^{-\theta}, 0) \tag{2.27}$$

with

$$\tilde{\chi}_{SG}(x, 0) \propto 1 - ax + o(x) \tag{2.28}$$

where a is a positive constant. The form (2.26) is derived as follows.

The correlation between S_i and S_j can be expressed by

$$\langle S_i S_j \rangle = \psi_g(i)\psi_g(j)\frac{Z_{++} - Z_{+-} - Z_{-+} + Z_{--}}{Z_{++} + Z_{+-} + Z_{-+} + Z_{--}} \tag{2.29}$$

where $\psi_g(i)$ is the value of the spin at the site i in one of the ground-state configurations, ψ_g, and $Z_{\pm\pm}$ is defined by

$$Z_{\pm\pm} \equiv \sum_{\psi \in \mathcal{S}_{\pm\pm}} \mathrm{e}^{-\beta E(\psi)}. \tag{2.30}$$

Here $E(\psi)$ is the total energy of a spin configuration ψ, and the $\mathcal{S}_{\pm\pm}$'s are sets of spin configurations defined by

$$\mathcal{S}_{\pm\pm} \equiv \{\psi | \psi \text{ is a spin configuration; } q(\psi, \psi_g) > 0; \quad \psi_g(i)\psi(i) = \pm 1; \\ \psi_g(j)\psi(j) = \pm 1\} \tag{2.31}$$

with

$$q(\psi, \psi') \equiv \frac{1}{N}\sum_i \psi(i)\psi'(i). \tag{2.32}$$

If the temperature is low enough to satisfy

$$TL^{-\theta} \ll J \tag{2.33}$$

we can neglect the contribution from the excited states which contain more than one excited droplet. Then, the restricted partition functions $Z_{\pm\pm}$ can be approximated by

$$Z_{++} \simeq \mathrm{e}^{-\beta E_g} \times \left(1 + \sum_{i \notin \mathcal{D}; j \notin \mathcal{D}}^{\mathcal{D}} \mathrm{e}^{-\beta E(\mathcal{D})}\right) \tag{2.34}$$

$$Z_{-+} \simeq \mathrm{e}^{-\beta E_g} \times \sum_{i \in \mathcal{D}; j \notin \mathcal{D}}^{\mathcal{D}} \mathrm{e}^{-\beta E(\mathcal{D})} \tag{2.35}$$

$$Z_{+-} \simeq \mathrm{e}^{-\beta E_g} \times \sum_{i \notin \mathcal{D}; j \in \mathcal{D}}^{\mathcal{D}} \mathrm{e}^{-\beta E(\mathcal{D})} \tag{2.36}$$

$$Z_{--} \simeq \mathrm{e}^{-\beta E_g} \times \sum_{i \in \mathcal{D}; j \in \mathcal{D}}^{\mathcal{D}} \mathrm{e}^{-\beta E(\mathcal{D})} \tag{2.37}$$

where $E(\mathcal{D})$ is the excitation energy of a droplet $\mathcal{D}$. Using the scaling form for the distribution function of the excitation energy of droplets of size l,

$$P(E, l) \simeq \frac{1}{\Upsilon l^{\theta}} \tilde{P}(E/l^{\theta}) \tag{2.38}$$

with

$$0 < \tilde{P}(0) \equiv \lim_{x \to 0} \tilde{P}(x) < \infty \tag{2.39}$$

we can evaluate these quantities as follows. Firstly, we have

$$[\zeta_{-+}]_J \equiv [\mathrm{e}^{\beta E_g} Z_{-+}]_J \simeq \sum_{\substack{\mathcal{D} \\ i\in\mathcal{D}, j\notin\mathcal{D}}} \mathrm{e}^{-\beta E(\mathcal{D})}$$
$$\simeq \sum_{n=0}^{\log R_{ij}/\log b} \int_0^\infty \mathrm{d}E P(E, b^n)\mathrm{e}^{-\beta E}$$
$$\simeq \sum_{n=0}^{\log R_{ij}/\log b} c' \frac{T}{b^{n\theta}} \simeq \frac{c}{8} T R_{ij}^{-\theta} \tag{2.40}$$

where c' and c are positive constants. We have assumed here that, if and only if the size of a droplet including the site i is greater than R_{ij}, it includes the site j. Similarly we have

$$[\zeta_{+-}]_J \equiv [\mathrm{e}^{\beta E_g} Z_{+-}]_J \simeq \tfrac{1}{8} c T R_{ij}^{-\theta}. \tag{2.41}$$

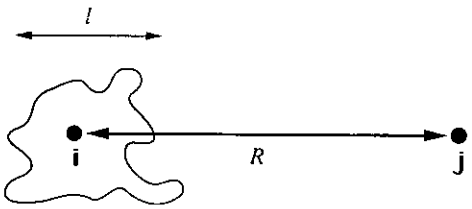

Figure 1. Two sites separated by the distance R and a droplet of size l.

Next, as for Z_{--} and Z_{++}, we have

$$[\zeta_{--}]_J \equiv [\mathrm{e}^{\beta E_g} Z_{--}]_J \simeq \sum_{n=\log R/\log b}^{\log L/\log b} c_{--} \frac{T}{b^{n\theta}} \simeq c_{--} T L^{-\theta} \tag{2.42}$$

and

$$[\zeta_{++}]_J - 1 \simeq [\mathrm{e}^{-\beta E(\mathcal{D}_L)}]_J \simeq c_{++} T L^{-\theta_S} \tag{2.43}$$

where $\mathcal{D}_L$ is the largest droplet which does not include i or j. Since we have assumed (2.33), the values of these four terms are small compared to unity, and we obtain

$$[\langle S_i S_j\rangle^2]_J = \left[\left(\frac{1+\zeta_{++}-\zeta_{+-}-\zeta_{-+}+\zeta_{--}}{1+\zeta_{++}+\zeta_{+-}+\zeta_{-+}+\zeta_{--}}\right)^2\right]_J$$
$$\simeq 1 - 8[\zeta_{+-}]_J \simeq 1 - cTR_{ij}^{-\theta} \tag{2.44}$$

which gives the asymptotic form (2.26).

3. Calculations of the nonlinear susceptibility and finite-size-scaling analysis

In the present section we develop scaling analysis for the zero-field spin-glass susceptibility. There are two methods for calculating this quantity; the transfer-matrix method and the Monte Carlo method. We have adopted the transfer-matrix method here, since it is very difficult to reach the scaling region by means of the Monte Carlo simulation [19].

It is difficult to calculate χ_{SG} directly from the definition of χ_{SG}

$$\chi_{SG} \equiv \frac{1}{N}\sum_{ij}[\langle S_i S_j\rangle^2]_J. \tag{3.1}$$

To obtain each correlation function $\langle S_i S_j\rangle$, we have to calculate the following quantity;

$$Z_{ij} \Leftarrow {}^t\mathbf{1}T_{L_y}T_{L_y-1}\cdots T_{j_y}S_j T_{j_y-1}\cdots T_{i_y}S_i T_{i_y-1}\cdots T_0\mathbf{1} \tag{3.2}$$

where T_{i_y} is the transfer-matrix which corresponds to tracing out all the spins in the i_y-th layer, and $\mathbf{1}$ denotes a 2^{L_x}-dimensional vector all of whose elements are unity. The calculation of χ_{SG} along this line requires about $N^2/2$ operations for each bond-configuration. It is much better to use the formula

$$\chi_{SG} = \tfrac{2}{3} - (1/6N)[\langle M^4\rangle - 3\langle M^2\rangle^2]_J. \tag{3.3}$$

Using the relation

$$[\langle M^4\rangle]_J = 3N^2 - 2N \tag{3.4}$$

we can further reduce the expression (3.3) as follows:

$$\chi_{SG} = \frac{1}{2N}[\langle M^2\rangle^2 - N^2]_J + 1. \tag{3.5}$$

We can use both the expressions (3.3) and (3.5) for the present purpose. The expression (3.5) has an advantage that we do not have to calculate the fourth moment $\langle M^4\rangle$. The calculation up to the nth order moment of M takes time proportional to n as is explained in the appendix. Thus the calculation through (3.5) takes only half of the computational time for (3.3). The right-hand side of (3.5) is, however, not self-averaging, that is, the ratio of these quantities before and after averaging over bond configurations

$$\lim_{N\to\infty}\frac{(\langle M^2\rangle^2 - N^2)/2N + 1}{[\langle M^2\rangle^2 - N^2]_J/2N + 1} \tag{3.6}$$

are not necessarily equal to unity. On the other hand, we have

$$\lim_{N\to\infty}\frac{(2/3) - \{\langle M^4\rangle - 3\langle M^2\rangle^2\}/6N}{(2/3) - [\langle M^4\rangle - 3\langle M^2\rangle^2]_J/6N} = 1 \tag{3.7}$$

which holds, because the quantity $\chi_2 = \beta^3(\langle M^4\rangle - 3\langle M^2\rangle^2)/6$ is self-averaging. In other words, if the system is large enough, the deviation concerning the average

operation in (3.5) becomes larger than that in (3.3). This may result in large errors of estimates of χ_{SG} through the expression (3.5). This is a disadvantage associated with (3.5). We have performed calculations of moments up to fourth order, and have used both the formulae (3.3) and (3.5). Two estimates agree with each other within the error bars, and in every case the errors in the first estimation given by (3.3) is a little smaller than that in the second estimation given by (3.5). The ratio of the errors is, for example, about $1.1 \sim 1.3$ for $L = 4 \sim 10$, and $T = 0.1 \sim 1.0 J/k_B$. In the present calculation we have used the data obtained through the expression (3.3). The algorithm for calculating higher moments is given in the appendix.

Calculations have been done for $L \times L$ systems which have a periodic boundary in one direction and a free boundary in the other. The parameters adopted in the calculations are listed in table 1. In figure 2, scaled data is plotted. We can see that the behaviour near $T = 0$ can be explained, very well, by the asymptotic form (2.14). Figure 2(*a*) shows a scaling plot with $\theta = -0.492$, which gives the best fitting to the data for $T \leqslant 0.6$ and $L \geqslant 6$. Figure 2(*b*) is the one using the values of θ obtained through the domain-wall scaling [8] ($\theta = \theta_S = -0.291$). Only a glance at these two figures is enough to see that the present data is not consistent with the estimate $\theta = -0.291$.

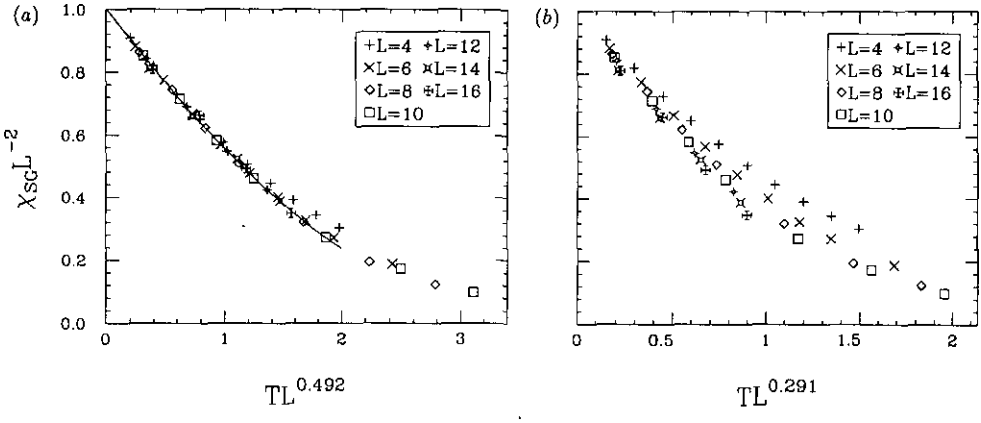

Figure 2. Scaling plots of spin-glass susceptibility $\chi_{SG}(T, 0, L)$ with (*a*) $\theta = -0.492$ and (*b*) $\theta = -0.291$, respectively. The statistical errors of data points are smaller than the size of symbols.

In order to obtain the best estimate of θ within the present data, we analysed them using the method of least squares. The fitting function we used is similar to (2.28), but includes two more higher-order terms

$$\chi_{SG} L^{-d} = 1 - (ax + bx^2 + cx^3) \tag{3.8}$$

where $x \equiv TL^{-\theta}$.

We have calculated the optimal value of θ, for which the chi-square is minimum. We have tried several selections of data in order to see how large the finite-size correction to scaling is. When we adopt the data for $0.1 \leqslant T \leqslant 0.6$, $4 \leqslant L \leqslant 16$, we get

$$-\theta = 0.524(4) \qquad S = 2.16 \qquad (T \leqslant 0.6; L \geqslant 4). \tag{3.9}$$

Table 1. The physical parameters and numbers of samples adopted in calculations of the zero-field spin-glass susceptibility χ_{SG}.

L	T	N_{smp}	L	T	N_{smp}	L	T	N_{smp}
4	0.1	1 000 000	6	0.1	1 000 000	8	0.1	1 000 000
4	0.2	1 000 000	6	0.2	1 000 000	8	0.2	1 000 000
4	0.3	1 000 000	6	0.3	1 000 000	8	0.3	1 000 000
4	0.4	1 000 000	6	0.4	1 000 000	8	0.4	1 000 000
4	0.5	1 000 000	6	0.5	1 000 000	8	0.6	60 000
4	0.6	500 000	6	0.6	100 000	8	0.8	10 000
4	0.7	500 000	6	0.7	100 000	8	1.0	10 000
4	0.8	500 000	6	0.8	50 000			
4	0.9	500 000	6	1.0	50 000			
4	1.0	500 000						
10	0.1	1 000 000	12	0.1	1 000 000	16	0.1	30 000
10	0.2	1 000 000	12	0.2	1 000 000	16	0.2	30 000
10	0.3	1 000 000	12	0.3	1 000 000	16	0.3	30 000
10	0.4	1 000 000	12	0.4	1 000 000	16	0.4	30 000
10	0.6	30 000	14	0.1	100 000			
10	0.8	3 000	14	0.2	100 000			
10	1.0	3 000	14	0.3	100 000			
			14	0.4	100 000			

Here S is the normalized chi-square defined by

$$S \equiv \frac{\sum(y_i - F_{fit}(x_i))^2}{n - m} \tag{3.10}$$

where n is the number of the data points and m is the number of the fitting parameters in the function F_{fit}. The figures in parentheses in (3.9) are estimates of the statistical errors which were obtained through the method of least-squares. When we adopt only the data for $0.1 \leqslant T \leqslant 0.6$ and $6 \leqslant L \leqslant 16$, we have

$$-\theta = 0.492(5) \qquad S = 1.19 \qquad (T \leqslant 0.6; L \geqslant 6). \tag{3.11}$$

For other selections we have obtained the following results:

$$-\theta = 0.478(10) \qquad S = 1.06 \qquad (T \leqslant 0.6; L \geqslant 8) \tag{3.12}$$

$$-\theta = 0.470(16) \qquad S = 1.01 \qquad (T \leqslant 0.6; L \geqslant 10) \tag{3.13}$$

$$-\theta = 0.490(40) \qquad S = 1.10 \qquad (T \leqslant 0.6; L \geqslant 12). \tag{3.14}$$

Further reduction of the number of the data points has given meaningless results. We should note that the error estimates here do not include the systematic error due to the finite-size effect. We can see that all the above estimates except for the first, (3.9), agree with each other within a margin for statistical error, and the values of the normalized chi-square S seem reasonable (near unity). From the above results, we conclude

$$-\theta = 0.48(1). \tag{3.15}$$

This value agrees with our previous estimate $-\theta = 0.476(5)$ (or $0.51(4)$) within the limit of statistical error.

4. CAM analysis of mean-field data

One difficulty in applying the finite-size scaling analysis to small clusters lies in the existence of finite-size correction to scaling. For example, there is ambiguity of the definition of the cluster size L in the finite-size scaling method: the system size may be defined by the edge length, by the number of sites on the edge, or by the total number of sites N as $L \equiv N^{1/d}$. The difference between them can affect the exponent estimation considerably, when we adopt the data from rather small systems. Such a type of correction may be expressed through the replacement of L by a continuous function $g(L)$. The coherent-anomaly method (CAM) [16] overcomes the difficulty as seen below.

If one measures a quantity $Q(T,0,L)$ at a temperature, say T_0, varying the system size L, but keeping the relation

$$T_0 L^{-\theta} = \text{constant} \tag{4.1}$$

(2.1) is followed by

$$Q(T_0,0,L) \propto T_0^{\psi_Q/\theta}. \tag{4.2}$$

The exponent ψ_Q/θ is nothing but the one which describes the singularity of the quantity in the thermodynamic limit; $Q(T,0,\infty) \propto T^{\psi_Q/\theta}$. Note that we eliminate the system size L from (4.1) by making the use of (4.1). It has been shown [16] that some systematic series of mean-field solutions $T_{\rm mf}(L)$ satisfy the condition (4.1) with $T_0 = T_{\rm mf}$. The double-cluster approximation (DCA) [13–15] is especially known to be tractable.

The detail of the formulation of the double-cluster approximation for spin glasses has been presented elsewhere [15]. Here we briefly review it emphasizing the scaling property [14]. Consider two clusters of size L_A and L_B. We apply a weak magnetic field H to the bulk of them and an effective field $H_{\rm eff}$ to the boundaries. We require the consistency condition $[\langle S_0\rangle_A^2]_J = [\langle S_0\rangle_B^2]_J$ to hold, where the symbol $\langle\cdots\rangle_A$ denotes the thermal average with respect to the Hamiltonian of the system A. The instability occurs at the temperature $T_{\rm D}(L_A,L_B)$ which satisfies the equation [15]

$$\Sigma(T_{\rm D},0,L_A) = \Sigma(T_{\rm D},0,L_B). \tag{4.3}$$

The subscript D indicates that $T_{\rm D}$ is the solution of the double-cluster approximation. The surface susceptibility Σ in (4.3) is defined by

$$\Sigma(T,0,L) \equiv \sum_{i\in\partial\tilde{\Omega}} [\langle S_0 S_i\rangle_L^2]_J \tag{4.4}$$

where the summation runs over the boundary sites of the cluster.

We can see [14] that the solution $T_{\rm D}$ satisfies the relation (4.1) with $T_0 = T_{\rm D}$, provided that

$$\Delta L \equiv |L_A - L_B| \ll L_A, L_B. \tag{4.5}$$

Assuming this condition we hereafter abbreviate the notation $T_{\rm D}(L_A,L_B)$ to $T_{\rm D}(L)$. Utilizing Fisher's finite-size scaling form (2.20), the surface susceptibility is estimated as

$$\Sigma(T,0,L) \propto L^{1-\eta} G(TL^{-\theta}). \tag{4.6}$$

The equation for T_D, under the condition (4.5), is reduced to the following expression, taking ΔL up to the first order; $\partial\Sigma/\partial L = 0$ at $T = T_D(L)$, or

$$0 = -(\partial/\partial L)\log\Sigma(T_D, 0, L) = L^{-1}D(T_D L^{-\theta}) \tag{4.7}$$

where

$$D(x) = \theta x\frac{G'(x)}{G(x)} - 1 + \eta. \tag{4.8}$$

The solution x_0 of the equation $D(x_0) = 0$ gives the relation

$$T_D(L)L^{-\theta} = x_0. \tag{4.9}$$

Therefore we can observe the behaviour (4.2) by adopting $T_D(L)$ as the temperature T_0.

Now we discuss here the relation (4.2) concretely for the two quantities, namely the critical amplitude $\overline{\chi}_{SG}$ of the mean-field susceptibility, and the bulk susceptibility χ_{SG}. First, the critical coefficient $\overline{\chi}_{SG}$ has been found [16] to follow the form (4.2). The mean-field susceptibility in the framework of the double-cluster approximation [15] is, up to the first order of ΔL, expressed as follows:

$$\begin{aligned}\chi_{SG}^{D} &= N\mu_B^4\frac{\Sigma(A)\chi_{SG}(B) - \chi_{SG}(A)\Sigma(B)}{\Sigma(A) - \Sigma(B)} \\ &\simeq -\frac{\Sigma}{(\partial/\partial L)\log\Sigma} \propto L^{2-\eta}\frac{G(TL^{-\theta})}{D(TL^{-\theta})}.\end{aligned} \tag{4.10}$$

Here we simplify the notation as $\chi_{SG}(T, 0, L_A) = \chi_{SG}(A)$. The critical coefficient $\overline{\chi}_{SG}$ defined by

$$\chi_{SG}^{D} \simeq \overline{\chi}_{SG}(T - T_D)^{-1} \tag{4.11}$$

shows the following behaviour:

$$\overline{\chi}_{SG} \propto T_D^{-\gamma_{SG}+1}H(x_0) \tag{4.12}$$

with

$$H(x) \equiv x^{\gamma_{SG}-1}\frac{G(x)}{D'(x)}. \tag{4.13}$$

It should be stressed here that the behaviour (4.12) remains unchanged even after we replace the variable L by $(L + a)$. This type of correction to the system size L may exist because of the ambiguity of the definition of L. The relations (4.9) and (4.10) are now changed to the forms $T_D(L + a)^{-\theta} = x_0$ and

$$\chi_{SG}^{D} \propto (L + a)^{2-\eta}\frac{G(T(L + a)^{-\theta})}{D(T(L + a)^{-\theta})} \tag{4.14}$$

and still we obtain the behaviour (4.12), owing to the elimination of the system size. Next, the bulk susceptibility χ_{SG} also behaves as (4.2), that is

$$\chi_{SG}(T_D(L), 0, L) \propto T_D^{-\gamma_{SG}} \int_0^{x_0} t^{\gamma_{SG}-1} G(t)\, dt. \tag{4.15}$$

This form is compatible with a more general type of correction to L than the one mentioned below (4.13); for example the replacement of L by $L(1 + aL^{-\omega} + \cdots)$.

Two of the present authors [15] analysed the two-dimensional $\pm J$ model, using the data $\{T_D, \overline{\chi}_{SG}\}$, and found that the clusters only up to 4×4 are enough to obtain such an estimate of γ_{SG} as is consistent with the ones by other authors. In the present paper we have used the clusters up to 6×6. The pairs of clusters used in the double-cluster approximation and the resulting data are listed together in table 2. The error estimation here has been done as follows. We have solved the equation (4.3) using the correlation data averaged over N_0 samples to obtain T_D and $\bar{\chi}$ (or χ_A, χ_B). The number N_0 is restricted by the amount of the computer memory and the job CPU-time limit. We have repeated this job N_1 times, renewing the set of samples. Finally, we have obtained the average and the error from the N_1 set of data. The total number of samples $N_0 N_1$ for each case is listed in table 2.

Table 2. The pairs of clusters used in the double-cluster approximation and the results; the mean-field critical temperature, the bulk susceptibility of the clusters, and the critical coefficient of the mean-field susceptibility. The figures in parentheses in the first and second columns show the round numbers of samples with the unit 10^6. The figures in parentheses in the other columns show the error estimates.

cluster A	cluster B	T_D	$\chi_{SG}(A)$	$\chi_{SG}(B)$	$\overline{\chi}_{SG}$
$2 \times 2(38)$	$2 \times 3(38)$	0.958 66(40)	2.119 86(56)	2.838 24(63)	2.347 37(72)
$2 \times 3(8)$	$3 \times 3(3)$	0.805 6(12)	3.188 0(31)	4.447 7(38)	3.437 7(55)
$3 \times 3(48)$	$3 \times 4(15)$	0.795 49(55)	4.490 5(25)	5.260 2(29)	3.513 6(43)
$3 \times 4(13)$	$4 \times 4(6)$	0.715 8(29)	5.745(20)	6.911(24)	4.688 9(65)
$4 \times 4(10)$	$4 \times 5(6)$	0.716 7(13)	6.904(12)	8.071(13)	4.683(12)
$4 \times 5(6)$	$5 \times 5(4)$	0.658 6(18)	8.767(23)	10.401(26)	6.025(23)
$5 \times 5(6)$	$5 \times 6(4)$	0.655 1(29)	10.456(49)	11.650(55)	6.081(32)
$5 \times 6(7)$	$6 \times 6(7)$	0.614 5(19)	12.475(41)	14.056(47)	7.476(31)
$2 \times 2(9)$	$3 \times 3(3)$	0.874 82(74)	2.228 4(10)	4.176 8(13)	2.826 5(16)
$2 \times 3(10)$	$3 \times 4(1)$	0.800 6(13)	3.200 2(33)	5.226 5(49)	3.468 0(64)
$3 \times 3(24)$	$4 \times 4(1)$	0.752 7(17)	4.672 9(84)	6.591(12)	4.053(10)
$3 \times 4(5)$	$4 \times 5(5)$	0.714 92(80)	5.751 27(59)	8.091 3(81)	4.692 6(63)
$4 \times 4(12)$	$5 \times 5(6)$	0.684 25(69)	7.200 8(69)	9.993 2(81)	5.318 6(39)
$4 \times 5(37)$	$5 \times 6(2)$	0.655 4(10)	8.807(13)	11.640(16)	6.052(15)
$5 \times 5(34)$	$6 \times 6(3)$	0.635 1(17)	10.782(32)	13.538(41)	6.717(23)

First, we have analysed the series $\{T_D, \overline{\chi}_{SG}\}$ by the method of least squares†. The log-log plot of the data is shown in figure 3. We have concluded that the condition (4.5) is practically satisfied. This conclusion has been drawn from the following fact, we have obtained the two series of data points; one for the pair of clusters $L_x \times L_y$

† In the least-squares analysis, the horizontal coordinate of the data points need to be given accurately. Owing to the necessity, we have used the data $\{T_D\}$ as the horizontal coordinates without errors, while we have added the properly scaled errors along the abscissa $\sigma(T_D) \times (\gamma_{SG} - 1)\overline{\chi}_{SG}/T_D$ to the errors along the ordinate $\sigma(\overline{\chi}_{SG})$.

and $L_x \times (L_y + 1)$, the other for the pair $L_x \times L_y$ and $(L_x + 1) \times (L_y + 1)$. We have observed that there is little discrepancy between the curves of the data sets $\{T_D, \overline{\chi}_{SG}\}$ for the two series. This means the correction term of the order $(\Delta L)^2$ is considerably small.

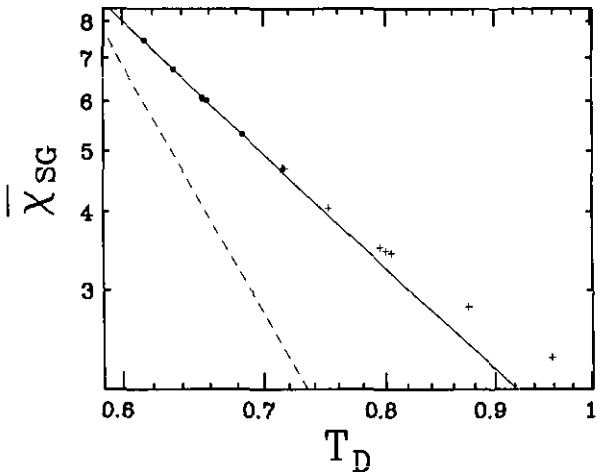

Figure 3. The log–log plots of T_D vs $\overline{\chi}_{SG}$. The errors of the data are comparable with the size of the symbols. The solid line shows the estimate (4.20). The dashed line is drawn for comparison so that the slope may correspond to the domain-wall scaling estimate $\theta = 0.291$ [7].

Since the data as a whole show apparent systematic deviation from the linear behaviour (4.12), we have tried to fit to all the data the function with higher-order correction terms

$$\overline{\chi}_{SG} = \sum_{n=1}^{N} c_n T_D^{-\gamma_{SG}+n}. \tag{4.16}$$

The result with $N = 3$ is

$$\gamma_{SG} = 4.56(54) \qquad S = 0.343$$
$$\text{(all the data with } N = 3). \tag{4.17}$$

Further increase of N has resulted in meaningless estimates with large errors. Then we have tried the fitting with $N = 1$ to selected data. The results are

$$\gamma_{SG} = 3.97(5) \qquad S = 0.625 \qquad (T_D < 0.76) \tag{4.18}$$
$$\gamma_{SG} = 4.00(6) \qquad S = 0.614 \qquad (T_D < 0.72) \tag{4.19}$$
$$\gamma_{SG} = 4.13(10) \qquad S = 0.204 \qquad (T_D < 0.69) \tag{4.20}$$
$$\gamma_{SG} = 4.2(2) \qquad S = 0.197 \qquad (T_D < 0.66). \tag{4.21}$$

Further reduction of the number of data points has resulted in a large error. Owing to the systematic deviation, the estimate tends to increase as we reduce the number of data points. Since the values of the normalized chi-square S are similar for (4.20) and (4.21), we consider that the series converge to the behaviour (4.12) in the region $T_D < 0.69$, which is specified by the six data points denoted by "•" in figure 3.

Next, we have analysed the data $\{T_D, \chi_{SG}(A)\}$ and $\{T_D, \chi_{SG}(B)\}$. The plots of the data show even-odd-oscillatory deviation from the expected behaviour. This fact

may be caused by the irregularity due to specific shapes of each cluster†. The series $\{T_D, \chi_{SG}(B)\}$ of the pairs $L_x \times L_y$ and $(L_x+1)\times(L_y+1)$ show the smoothest behaviour (figure 4). We have fitted the function (4.15) to this series rejecting only the data (2×2)-(3×3), which deviates apparently from the linear behaviour. The result is

$$\gamma_{SG} = 4.13(5) \qquad S = 5.43 \qquad (T_D < 0.81) \tag{4.22}$$

or the solid line in figure 4. This estimate is consistent with (4.20). The normalized chi-square is greater than unity, which is caused by the oscillatory behaviour of the whole series. This may imply a hidden systematic error in this estimation.

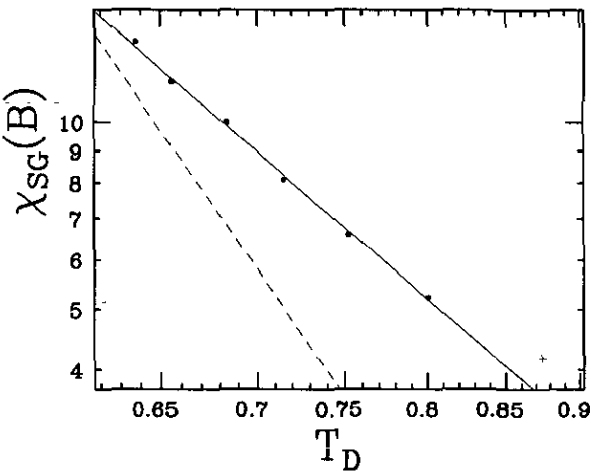

Figure 4. The log-log plots of T_D vs $\chi_{SG}(B)$. The errors of the data are comparable with the size of the symbols. Only the series with the pairs of $L_x \times L_y$ and $(L_x+1)\times(L_y+1)$ are shown. The solid line corresponds to the estimate (4.22), while the dashed line, $\theta = 0.291$ [7].

Based on the estimates (4.17), (4.20) and (4.22), we conclude the present section with the following estimate (the solid line in figure 3)

$$\gamma_{SG} = 4.13(10) \qquad \text{or} \qquad -\theta = d/\gamma_{SG} = 0.484(12). \tag{4.23}$$

This agrees with the estimate (3.15) very well. For comparison we have drawn in figure 3 and figure 4 the dashed lines corresponding to the domain-wall-scaling estimate $-\theta = -\theta_S = 0.291$ [7]. In both the figures, the present data is not consistent with these lines.

5. Discussion and summary

In the present paper, we have obtained new estimates of the exponent $-\theta \equiv 1/\nu$ through calculations of the zero-field spin-glass susceptibility, in order to confirm the previous estimation through the calculation of the zero-temperature magnetization.

We have performed two kinds of calculations of χ_{SG}. Both of them have been performed by the numerical transfer-matrix method. The first is the direct calculation of the nonlinear susceptibility. The exponent $1/\nu$ has been obtained through the

† On the other hand, the data $\{T_D, \overline{\chi}_{SG}\}$ give rather smooth behaviour. Though the reason of the difference is not clear, we suggest that the irregularity of the function $G(x)$ may be partially cancelled between the denominator and the numerator of (4.13)

finite-size-scaling analysis assuming the asymptotic behaviour of $\tilde{\chi}_{SG}$ predicted by the droplet argument. The data confirm the prediction well. The critical exponent obtained in this scheme is

$$-\theta = 1/\nu = 0.48(1). \tag{5.1}$$

The second is the mean-field calculation analysed by the coherent-anomaly method. The method is based on Fisher's finite-size scaling form (2.20), which is compatible with (2.14). The exponent estimate γ_{SG} thus obtained is

$$\gamma_{SG} = 4.13(10) \simeq 2/0.484(12). \tag{5.2}$$

This is fully consistent with (5.1) via the scaling relation (2.16).

Generally speaking, we cannot objectively exclude the possibility that further calculation may reveal a systematic error of the present estimates. We believe, however, that finite-size correction does not affect the present results so much. There are three reasons for this. Firstly, both the scaling plot and the CAM plot are fitted well. This fact suggests that irregularity caused by specific shapes of the clusters is irrelevant in the present estimates. Secondly, the present two estimates are consistent with each other, while the estimate in section 4 is expected to be partly free from finite-size correction. This suggests that the correction to scaling which can be expressed in terms of the simple replacement of L by $g(L)$ is irrelevant here. Thirdly the estimates (5.1) and (5.2) agree with the previous estimate (1.5) [12]. Note that the present estimation and the previous one are complementary to each other. The previous study dealt with the criticality at $T = 0$ and $H \to 0$, while the present one, at $H = 0$ and $T \to 0$.

Since the exponents ν and γ_{SG} estimated here are directly related to the temperature-scaling exponent θ, the disagreement between our results and the ones by other authors (1.1) [8] and (1.2) [9] suggests that the assumption $\theta = \theta_S$ in the domain-wall scaling does not hold in the present model. It is also puzzling that our results are inconsistent with the previous estimates [10, 11] through analyses of eigenvalues of transfer matrices. We believe that more consideration on the effect of the fractal dimension of the domain walls is required for more complete understanding.

Acknowledgments

The authors are grateful to Professor Y Kanada for useful comments on numerical calculations. The calculations were performed preliminarily on VAX6440 of the Meson Science Laboratory, Faculty of Science, University of Tokyo, and mainly on HITAC S820/80E of Kanagawa Works, Hitachi Corporation. We thank these facilities.

Appendix. Calculation of higher-order moments through the transfer-matrix method

In this appendix, we describe an algorithm of the transfer-matrix method for high-order moments. For simplicity of our explanation, let us consider a two-dimensional lattice of size $L_x \times L_y$. The extension to higher-dimensional systems is straightforward. Our task is to calculate

$$Z_\mu \equiv \mathrm{Tr}(\mathrm{e}^{-\beta\mathcal{H}} M^\mu) \qquad (\mu = 0, 1, 2, 3, \ldots) \tag{A.1}$$

where

$$\mathcal{H} \equiv -\sum_{i_x=1}^{L_x}\sum_{i_y=1}^{L_y}\{J^x_{(i_x,i_y)}S_{(i_x,i_y)}S_{(i_x+1,i_y)} + J^y_{(i_x,i_y)}S_{(i_x,i_y)}S_{(i_x,i_y+1)} + H_{(i_x,i_y)}S_{(i_x,i_y)}\} \tag{A.2}$$

and

$$M \equiv \sum_{(i_x,i_y)} S_{(i_x,i_y)}. \tag{A.3}$$

Assume that the boundary condition in the y direction is free ($J_{(i_x,L_y)} = 0$). Consider a 2^{L_x}-dimensional vector space in which every element of a vector is specified by an L_x-bit integer, ψ

$$\psi \equiv (\psi_{L_x}, \psi_{L_x-1}, \ldots, \psi_1) \equiv \sum_{i_x=1}^{L_x} 2^{i_x-1}\psi_{i_x} \qquad (\psi_{i_x} = 0, 1). \tag{A.4}$$

Next let us define transfer matrices as follows:

$$V_{i_x,i_y}(\psi'|\psi) \equiv \begin{cases} \exp(v_{i_x,i_y}) & (\psi' \oplus \psi = 0) \\ \exp(-v_{i_x,i_y}) & (\psi' \oplus \psi = 2^{i_x-1}) \\ 0 & \text{otherwise} \end{cases} \tag{A.5}$$

$$H_{i_x,i_y}(\psi'|\psi) \equiv \begin{cases} \exp(h_{i_x,i_y}) & (\psi' \oplus \psi = 0; \psi_{i_x} = \psi_{i_x+1}) \\ \exp(-h_{i_x,i_y}) & (\psi' \oplus \psi = 0; \psi_{i_x} = 1 - \psi_{i_x+1}) \\ 0 & \text{otherwise} \end{cases} \tag{A.6}$$

$$F_{i_x,i_y}(\psi'|\psi) \equiv \begin{cases} \exp(f_{i_x,i_y}) & (\psi' \oplus \psi = 0; \psi_{i_x} = 1) \\ \exp(-f_{i_x,i_y}) & (\psi' \oplus \psi = 0; \psi_{i_x} = 0) \\ 0 & \text{otherwise} \end{cases} \tag{A.7}$$

and

$$S_{i_x}(\psi'|\psi) \equiv \begin{cases} +1 & (\psi' \oplus \psi = 0; \psi_{i_x} = 1) \\ -1 & (\psi' \oplus \psi = 0; \psi_{i_x} = 0) \\ 0 & \text{otherwise} \end{cases} \tag{A.8}$$

where

$$v_{(i_x,i_y)} \equiv \beta J^y_{(i_x,i_y)} \tag{A.9}$$

$$h_{(i_x,i_y)} \equiv \beta J^x_{(i_x,i_y)} \tag{A.10}$$

and

$$f_{(i_x,i_y)} \equiv \beta H_{(i_x,i_y)}. \tag{A.11}$$

The symbol $\oplus$ denotes bit-wise exclusive-or operation. Then the partition functions Z_μ can be written in the form

$$Z_\mu \equiv {}^t\mathbf{1}(\sum_{i_y}\hat{S}_{i_y})^\mu F_{L_y}H_{L_y}V_{L_y-1}F_{L_y-1}H_{L_y-1}V_{L_y-2}F_{L_y-2}\cdots V_1F_1H_1\mathbf{1}. \tag{A.12}$$

Here

$$V_{i_y} \equiv \prod_{i_x} V_{i_x,i_y} \tag{A.13}$$

$$H_{i_y} \equiv \prod_{i_x} H_{i_x,i_y} \tag{A.14}$$

$$F_{i_y} \equiv \prod_{i_x} F_{i_x,i_y} \tag{A.15}$$

and $\hat{S}_{i_y}$ is an operator which transforms F_{i_y} into SF_{i_y}, where $S \equiv \sum_{i_x=1}^{L_x} S_{i_x}$. The symbol $\mathbf{1}$ stands for the vector all of whose elements are unity. The algorithm for calculating $Z_0, Z_1, \cdots$ and Z_μ is as follows.

(1) $\boldsymbol{w}^{(0)} \Leftarrow F_1 H_1 \mathbf{1}$.
(2) For $\alpha = 1$ to $\alpha = \mu$, do

$$\boldsymbol{w}^{(\alpha)} \Leftarrow \frac{1}{\alpha!} S^\alpha \boldsymbol{w}^{(0)}. \tag{A.16}$$

(3) For $i_y = 0$ to $i_y = L_y$, do
(a) For $\alpha = 0$ to $\alpha = \mu$, do

$$\boldsymbol{w}^{(\alpha)} \Leftarrow F_{i_y+1} H_{i_y+1} V_{i_y} \boldsymbol{w}^{(\alpha)}. \tag{A.17}$$

(b) For $\alpha = 1$ to $\alpha = \mu$, do

$$\boldsymbol{v}^{(\alpha)} \Leftarrow \sum_{\nu=0}^{\alpha} \frac{1}{\nu!} S^\nu \boldsymbol{w}^{(\alpha-\nu)}. \tag{A.18}$$

(c) For $\alpha = 1$ to $\alpha = \mu$, do

$$\boldsymbol{w}^{(\alpha)} \Leftarrow \boldsymbol{v}^{(\alpha)}. \tag{A.19}$$

(4) For $\alpha = 0$ to $\alpha = \mu$, do

$$Z_\alpha \Leftarrow \alpha!^t \mathbf{1} \boldsymbol{w}^{(\alpha)}. \tag{A.20}$$

For a finite μ, the most time-consuming part of the above procedure is obviously step 3(a) if L_x is large. Therefore the computational time is proportional to μ, namely the highest degree of the moment which we wish to calculate.

References

[1] Fisher D S and Huse D A 1988 *Phys. Rev.* B **38** 386
[2] Bhatt R N and Young A P 1988 *Phys. Rev.* B **37** 5606
[3] Ogielski A T 1985 *Phys. Rev.* B **32** 7384
[4] Caracciolo S, Parisi G, Patarnello and Sourlas N 1990 *J. Phys.* **51** 1877
[5] Kawashima N, Ito N and Suzuki M 1992 *J. Phys. Soc. Japan* **61** 1777

[6] Bhatt R N and Young A P 1986 *Heidelberg Colloquium on Glassy Dynamics* ed J L van Hemmen and I Morgenstern (Berlin: Springer)
[7] Bray A J and Moore M A 1986 *Heidelberg Colloquium on Glassy Dynamics* ed J L van Hemmen and I Morgenstern (Berlin: Springer)
[8] Bray A J and Moore M A 1984 *J. Phys. C: Solid State Phys.* 17 L463
[9] McMillan W L 1984 *Phys. Rev.* B **30** 476
[10] Cheung H F and McMillan W L 1983 *J. Phys. C: Solid State Phys.* **16** 7033
[11] Huse D A and Morgenstern I 1985 *Phys. Rev.* B **32** 3032
[12] Kawashima N and Suzuki M 1992 *J. Phys. A: Math. Gen.* **25** 1055
[13] Oguchi T and Kitatani H 1988 *J. Phys. Soc. Japan* **57** 3973
[14] Suzuki M, Hatano N and Nonomura Y 1991 *J. Phys. Soc. Japan* **60** 3990
[15] Hatano N and Suzuki M 1992 *J. Stat. Phys.* **66** 897
[16] Suzuki M 1991 *Evolutionary Trends in the Physical Sciences* ed M Suzuki and R Kubo (Berlin: Springer) and references therein
[17] Suzuki M 1977 *Prog. Theor. Phys.* **58** 1151
[18] Kawamura H *preprint*
[19] Morgenstern I and Binder K 1980 *Phys. Rev.* B **22** 288